Acta Cryst E
CRYSTALLOGRAPHIC COMMUNICATIONS
ISSN 2056-9890

Structure of racemic calcium 5-methyltetrahydrofolate trihydrate from synchrotron powder diffraction data and density functional theory

Jacob K. Salazar and James A. Kaduk*

Department of Chemistry, North Central College, 131 S. Loomis, St., Naperville IL, 60540 , USA. *Correspondence e-mail: kaduk@polycrystallography.com

Received 22 October 2025
Accepted 24 November 2025

Edited by W. T. A. Harrison, University of Aberdeen, United Kingdom

Keywords: powder diffraction; 5-methyltetrahydrofolate calcium; Metafolin; Rietveld refinement; density functional theory.

CCDC references: 2505413; 2505412

Supporting information: this article has supporting information at journals.iucr.org/e

The crystal structure of the racemic title compound, poly[[(μ-(2*S*)-2-{[4-({[(6*S*)-2-amino-5-methyl-1,4,5,6,7,8-hexahydropteridin-6-yl]methyl}amino)phenyl]-formamido}pentanedioato)diaquacalcium(II)] monohydrate], $\{[Ca(C_{20}H_{23}N_7O_6)(H_2O)_2]\cdot H_2O\}_n$ (space group $P2_1/c$) has been solved and refined using synchrotron X-ray powder diffraction data and optimized using density functional theory techniques. The structure consists of alternating hydrophilic (Ca/O) and hydrophobic layers lying parallel to the *bc* plane. An extensive network of O—H···O hydrogen bonds link the Ca coordination spheres within the layers. The anions link the Ca^{2+} ions into chains propagating along the *b*-axis direction. N—H···O hydrogen bonds link the Ca/O units and the anion layers. The calcium ion is 6-coordinate (distorted octahedral), and is isolated. The coordination sphere consists of two water molecules, a chelated carboxylate group, a monodentate carboxylate group, and a carbonyl group. Both the Ca coordination geometry and the extended structure are very different than that of the previously determined enantiopure calcium L-5-methyltetrahydrofolate trihydrate (Form I).

1. Chemical context

Levomefolic acid is a metabolite of folic acid (Vitamin B9), and is a major active form of folate found in foods and in the blood circulation. It is transported across membranes, including the blood-brain barrier. It plays an essential role in DNA and protein synthesis. Levomefolate is approved as a food additive, and is designated as a GRAS (generally recognized as safe) compound. Levomefolate plays major roles in the prevention of birth defects and the formation of red blood cells, which prevents anemia, and has been linked to support for cognitive and mental health. Folic acid deficiency can cause neural tube defects in fetuses and irreversible nervous system damage when combined with vitamin B12 deficiency. It is available commercially as a crystalline calcium salt (trade name Metafolin), which has the required stability for use as a supplement (https://www.drugbank.ca/salts/DBSALY001276). The IUPAC name (CAS Registry number 151533-22-1 for the anhydrous salt) is (2*S*)-2-[(4-{[(6*S*)-2-amino-5-methyl-4-oxo-3,6,7,8-tetrahydropteridin-6-yl]methyl-amino}benzoyl)amino]pentanedioate calcium trihydrate.

Stable crystalline salts of 5-methyltetrahydrofolic acid are disclosed and claimed in US Patent 6,441,168 (Müller *et al.*, 2002; Eprova AG). The patent includes X-ray powder diffraction data for crystalline Types I–IV of calcium L-5-methyltetrahydrofolate, as well as the amorphous form. The patent includes claims for 'a water of crystallization of at least one equivalent per equivalent of 5-methyltetrahydrofolic acid'

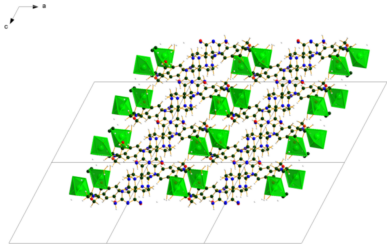

OPEN ACCESS
Published under a CC BY 4.0 licence

and '≥3 equivalents of water'. Commercial samples are generally described as the trihydrate, although the pentahydrate is also available commercially.

The powder pattern of a sample of calcium L-5-methyltetrahydrofolate trihydrate, (**I**), did not correspond to those of Type I (Müller *et al.*, 2002; Kaduk *et al.*, 2023) or any other reported form of the compound. A laboratory pattern could be indexed on a primitive monoclinic unit cell with a = 15.944 (11), b = 11.364 (6), c = 15.409 (6) Å, β = 118.52 (2)°, V = 2453.1 (33) Å^3, and Z = 4. The suggested space group by *FOX* (Favre-Nicolin and Černý, 2002) was $P2_1/c$, which is impossible for a chiral molecule, and led us to conclude that the sample was racemic.

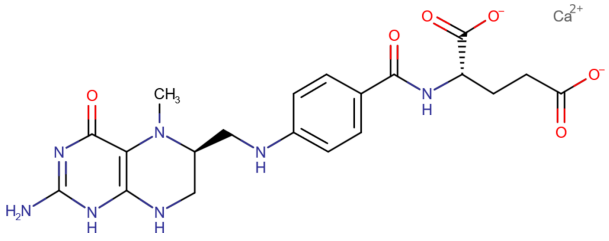

2. Structural commentary

The synchrotron powder pattern of (**I**) does not correspond to that of the intended Form I (Fig. 1, Kaduk *et al.*, 2023). Solution and refinement of the structure in the centrosymmetric space group $P2_1/c$ confirms that it is a racemate instead of the intended enantiopure material. In the arbitrarily-chosen asymmetric unit, atoms C14 and C25 have *S* configuration, but crystal symmetry generates the other enantiomer.

The root-mean-square (r.m.s.) difference of the non-H atoms in the Rietveld-refined and VASP-optimized structures of (**I**) calculated using the *Mercury* Calculate/Molecule Overlay tool, is 1.373 Å (Fig. 2). The agreement is outside the normal range for correct structures (van de Streek & Neumann, 2014). This large structure, refined using limited data, would be expected to be less accurate than usual. The

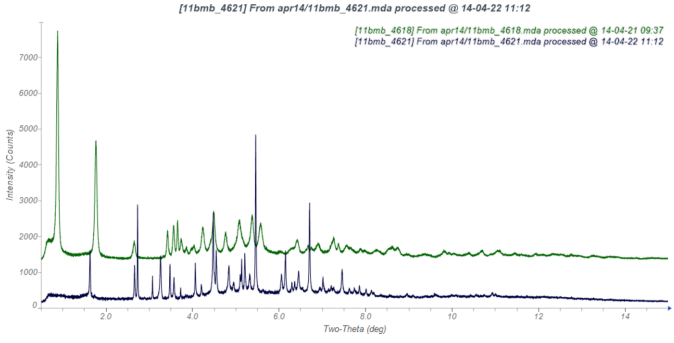

Figure 1
Comparison of the synchrotron diffraction pattern of (**I**) (black) to that of Form I of calcium L-5-methyltetrahydrofolate trihydrate reported by Müller *et al.* (2002; green). The patent pattern (measured using Cu K_α radiation) was digitized using *UN-SCAN-IT* (Silk Scientific, 2013) and converted to the synchrotron wavelength of 0.413691 (2) Å using *JADE Pro* (MDI, 2025).

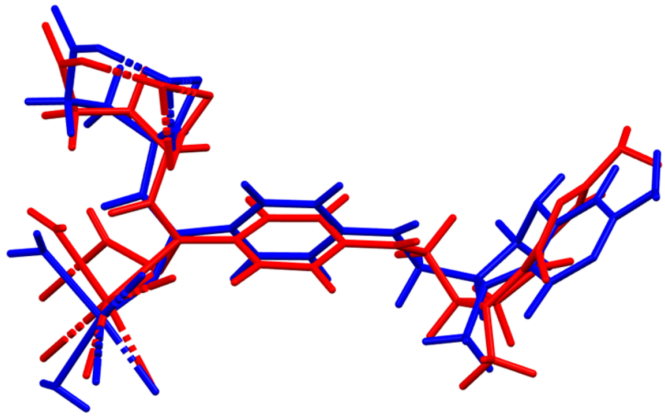

Figure 2
Comparison of the Rietveld-refined structure of (**I**) (red) to the *VASP*-optimized structure (blue). The comparison was generated using the *Mercury* Calculate Molecule Overlay tool; the r.m.s. difference is 1.373 A.

asymmetric unit is illustrated in Fig. 3. The refined structure has a close contact between C30 and Ca34, which is relieved on optimization. The U_{iso} values of the atoms in the side chain are very large, perhaps indicating disorder. Because the VASP optimization requires an ordered model, we prefer to not attempt to model any disorder. The remaining discussion will emphasize the VASP-optimized structure.

Most of the bond distances, bond angles, and torsion angles for (**I**) fall within the normal ranges indicated by a *Mercury* Mogul Geometry check (Macrae *et al.*, 2020). The C30—O2 bond length of 1.290 Å [average = 1.240 (15) Å, Z-score = 3.4] and the C18—N8 bond of 1.377 Å [average = 1.322 (10) Å, Z-score = 5.4] are flagged as unusual. The uncertainties on these averages are relatively low, inflating the Z-scores, and only a few similar hits were found. No hits were found for the angles O3—C32—C25, O4—C32—C25, and O5—C33—O6, suggesting that the coordination of the anion to the calcium ion is unusual. The angles C15—C14—N7 [114.0°, average = 108.9 (11)°, Z-score = 4.5] and C15—N8—C18 [113.1°,

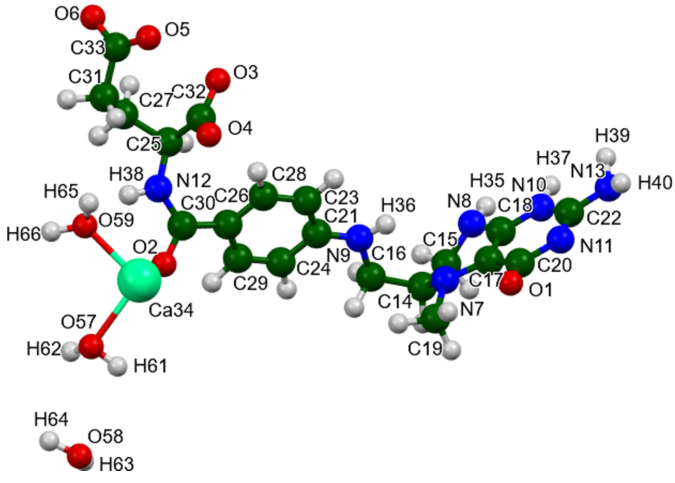

Figure 3
The asymmetric unit of (**I**) with the atom numbering. Image generated using *Mercury* (Macrae *et al.*, 2020).

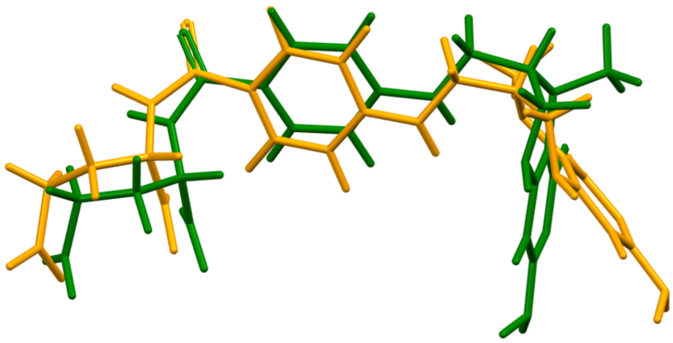

Figure 4
Comparison of the observed structure of the 5-methyltetrahydrofolate anion (orange) to that of a local minimum (green). The r.m.s. difference is 1.284 Å.

average = 120.1 (4), *Z*-score = 19.1, 2 hits] are flagged as unusual. The uncertainties on both averages are very low, inflating the *Z*-scores. Torsion angles involving rotation about the C30—N12 amide bond lie on the tails of planar distributions. Torsion angles involving rotation about the C14—C16 bond (which reflect the orientation of the fused ring system and the phenyl group) lie on the tails of *gauche/trans* distributions. Both sets of torsion angles are thus slightly unusual.

The Ca^{2+} ion is 6-coordinate (distorted octahedral), and is isolated. The bond-valence sum is 2.12. The average deviation from the ideal octahedral angles is 14.5 (122)°, and the median deviation is 11.1°. The coordination sphere consists of two water molecules, a chelated carboxylate group O3—C32—O4, a monodentate carboxylate group O5, and a carbonyl group O2. A connectivity search of this coordinate sphere in the Cambridge Structural Database (CSD; Groom *et al.*, 2016) yielded five hits. CSD refcode FOZDAB (Okamura *et al.*, 2015) has disordered Ca cations. In the other four [LOBXAE (Das, 2019), LOMMIJ (Acharya *et al.*, 2000), PIBSOJ (Cotter *et al.*, 2007), and WUKZOU (Hong *et al.*, 2020], one O atom of the chelating carboxylate group also bonds to an adjacent calcium cation. The Ca^{2+} coordination in this structure is unique.

Quantum chemical geometry optimization of the isolated 5-methyltetrahydrofolate anion (DFT/B3LYP/6-31G*/water) using *Spartan '24* (Wavefunction, 2025) indicated that the observed conformation is 9.6 kJ mol^{-1} higher in energy than a local minimum (Fig. 4). The r.m.s. Cartesian displacement between the structures is 1.284 Å. The differences are spread throughout the anion, but are most pronounced in the orientation of the tetrahydropteridin ring system. The global minimum-energy conformation (MMFF force field) is 144.7 kJ mol^{-1} lower in energy, and is much more compact; the anion folds upon itself to make the phenyl and tetrahydropteridin ring systems parallel and to form intramolecular hydrogen bonds. Intermolecular interactions are clearly important to determining the observed solid-state conformation.

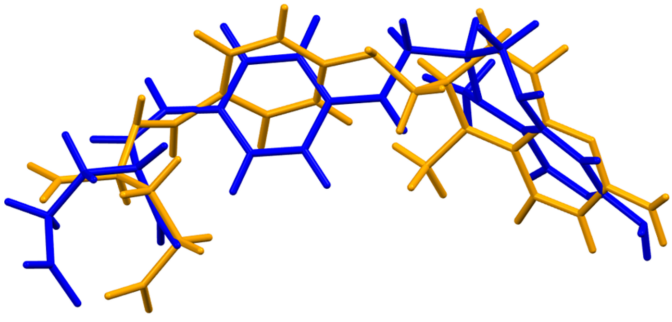

Figure 5
Comparison of the structure of the anion in (**I**) (blue) to that in enantiopure Type I (orange). The r.m.s. difference is 1.752 Å.

Table 1
Hydrogen-bond geometry (Å, °) for I_VASP.

D—H···*A*	*D*—H	H···*A*	*D*···*A*	*D*—H···*A*
N8—H35···O57^{i}	1.02	2.48	3.490	169
N10—H37···O3^{ii}	1.03	1.85	2.805	152
N12—H38···O59	1.03	2.00	2.991	160
N13—H39···O3^{ii}	1.03	2.21	2.928	125
N13—H39···O1^{iii}	1.03	2.34	3.086	128
O57—H61···O4^{iv}	0.98	2.24	2.888	122
O57—H62···O2^{v}	1.01	1.62	2.625	176
O58—H64···O5^{vi}	1.00	1.81	2.749	156
O59—H65···O58^{v}	1.00	1.66	2.588	151
O59—H66···O6^{vii}	1.04	1.49	2.525	170
C16—H45···O1^{viii}	1.10	2.47	3.349	136
C19—H48···O1	1.09	2.06	2.791	121
C24—H50···O1^{viii}	1.09	2.14	3.157	154
C25—H51···N13^{ix}	1.10	2.22	3.120	137
C28—H54···O4	1.09	2.28	3.263	150
C31—H60···O58^{v}	1.10	2.37	3.446	165

Symmetry codes: (i) $x-1, y, z$; (ii) $-x, y+\frac{1}{2}, -z+\frac{3}{2}$; (iii) $-x, -y+1, -z+2$; (iv) $-x+1, y+\frac{1}{2}, -z+\frac{3}{2}$; (v) $-x+1, -y+1, -z+1$; (vi) $x, -y+\frac{1}{2}, z-\frac{1}{2}$; (vii) $-x+1, -y, -z+1$; (viii) $x, -y+\frac{3}{2}, z-\frac{1}{2}$; (ix) $-x, y-\frac{1}{2}, -z+\frac{3}{2}$.

This racemate is 5687.0 kJ mol^{-1} cell^{-1} lower in VASP energy than the previous enantiopure structure (Kaduk *et al.*, 2023), even though the unit-cell volumes *V*(rac) = 2532.84 and *V*(old) = 2523.58 Å^3, and thus the densities (1.446 and 1.453 g cm^{-3}, respectively) are similar. The r.m.s. difference is 1.752 Å (Fig. 5), and the previously determined anion is 67.7 kJ mol^{-1} lower in energy. In this structure each anion coordinates to two Ca^{2+} cations, while in the previous structure each anion coordinates to four Ca^{2+} ions.

In (**I**), the Ca^{2+} ion is 6-coordinate; the coordination sphere consists of one chelated carboxyl group (O3 and O4), one monodentate carboxyl group (O5, which results in a triple chelation to the Ca), a carbonyl group, and two water molecules. In the previous structure the calcium ion is 7-coordinate; the coordination sphere consists of one chelated carboxyl group: O5 and O6, four mondentate carboxyl groups (O3, O4, O5, and O6), and one water molecule. In this structure the Ca^{2+} ion are isolated, while in the previous structure the calcium ions form one-dimensional chains. In this structure there is one isolated water molecule, while in the previous structure there are two.

In this structure there are five independent O—H···O hydrogen bonds (Table 1), while in the previous structure there are only three. Likewise there are four and two N—H···O hydrogen bonds, and one and three N—H···N hydrogen bonds. respectively. We suspect that the hydrogen bonds are the principal contributors to the lower energy of this structure.

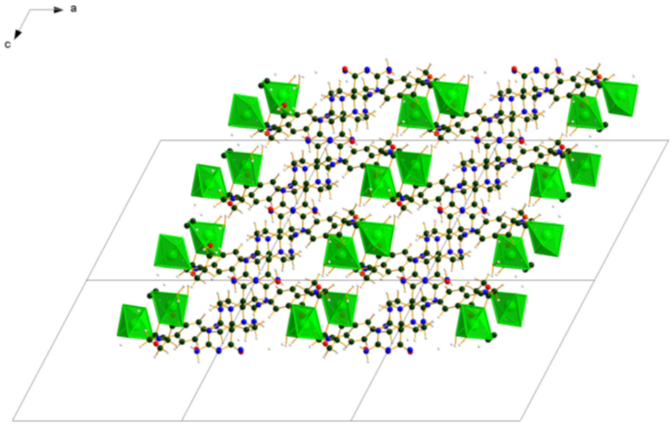

Figure 6
The crystal structure of (**I**) viewed down the *b*-axis direction.

3. Supramolecular features

The crystal structure of (**I**) (Fig. 6) consists of alternating hydrophilic (Ca/O) and hydrophobic layers lying parallel to the *bc* plane. An extensive network of O—H···O hydrogen bonds (Table 1) link the Ca coordination spheres within the layers (Fig. 7). Anions link Ca into chains along the *b*-axis (Fig. 8) and N10/N13—H···O3 hydrogen bonds link the Ca/O and anion layers (Fig. 9).

Since both carboxyl groups coordinate to Ca, they make up the outer surface of the 'hydrophilic' layer. In the center of these layers, the C/N ring systems interleave in a complex manner (Fig. 10). The closest phenyl–tetrahydropteridin distance is 4.71 Å (centroids), and the shortest tetrahydropteridin–tetrahydropteridin distance is 6.45 Å. The *Mercury* Aromatics Analyser indicates only weak interactions between phenyl rings, with distances > 6.8 Å.

Analysis of the contributions to the total crystal energy of the structure using the Forcite module of *Materials Studio* (Dassault Systèmes, 2024) indicated that the intramolecular energy is dominated by angle distortion terms, as expected for a system containing fused rings. The intermolecular energy is small, and consists mainly of van der Waals attractions. The hydrogen bonds are better discussed using the results of the DFT calculation.

Hydrogen bonds (Table 1) are important in the crystal structure of (**I**). The coordinated water molecule O57 acts as a donor to an 'intramolecular' carboxylate O4 atom and to the coordinated carbonyl group O2. The coordinated water molecule O59 acts as a donor in two very strong hydrogen bonds to the carboxylate O6 and the free water molecule O58. The energies of the O—H···O hydrogen bonds were calculated using the correlation of Rammohan & Kaduk (2018). The uncoordinated water molecule O58 makes a strong O—H···O hydrogen bond to the carboxylate O5, and makes bifurcated O—H···(C,C) hydrogen bonds to the phenyl ring atoms C24 and C29, *i.e.*, an O—H···π link. These are among the most negatively charged C atoms in the anion.

As noted above, the N10/N13—H37/H39···O3 hydrogen bonds link the Ca/O and anion layers from the tetrahydropteridin ring systems and one of the carboxylate O atoms. The amide N12 atom makes a strong intramolecular N—H···O hydrogen bond to the coordinated water molecule O59. The ring N8 atom makes a weaker intermolecular hydrogen bond

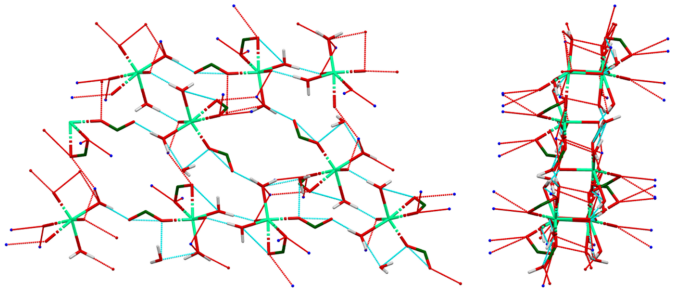

Figure 7
The O—H···O hydrogen-bonded layers in (**I**). On the left is a view down the *a*-axis, and on the right is a view down the *c*-axis.

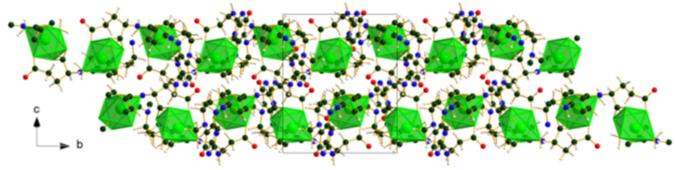

Figure 8
The hydrogen-bonded chains of Ca^{2+} cations propagating along the *b*-axis direction.

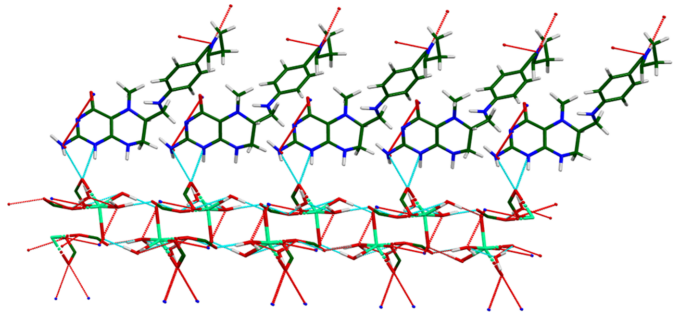

Figure 9
The N—H···O hydrogen bonds, which link the hydrophobic and hydrophilic layers in the extended structure of (**I**).

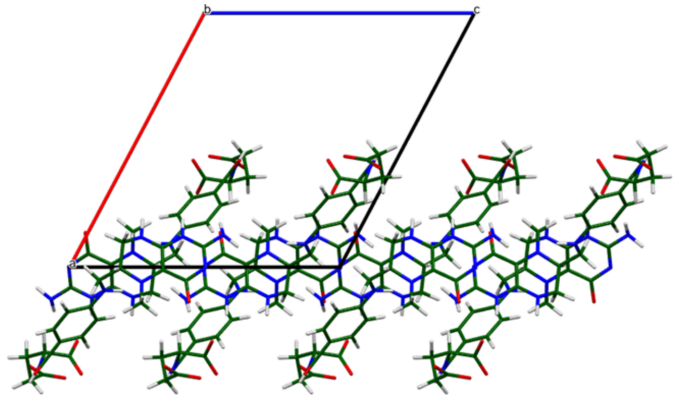

Figure 10
The interleaving of the aromatic ring systems in the extended structure of (**I**).

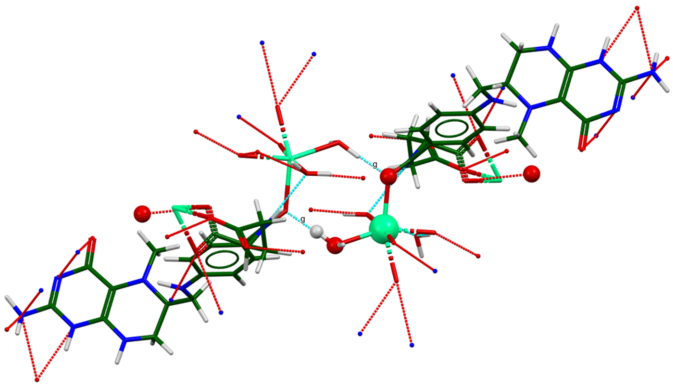

Figure 11
The $R_2^2(8)$ ring pattern that links the Ca^{2+} cations in the extended structure of (**I**).

to the coordinated water molecule O57. The energies of the N—H···O hydrogen bonds were calculated using the correlation of Wheatley & Kaduk (2019). There is an intramolecular N9—H36···N7 hydrogen bond. Several C—H···O and two C—H···N hydrogen bonds also contribute to the cohesion of the structure.

Although the Ca coordination spheres are isolated (*i.e.*, they do not share corners, edges, or faces), they are linked by a centrosymmetric pair of O57—H62···O2 hydrogen bonds between one of the coordinated water molecules and the coordinated carbonyl group. This ring pattern (Fig. 11) has the graph-set (Etter, 1990) motif $R_2^2(8)$. N8 and N10 participate in the same $R_2^2(8)$ pattern, which links the anion and the Ca coordination sphere (Fig. 12).

The Bravais–Friedel–Donnay–Harker (Bravais, 1866; Friedel, 1907; Donnay & Harker, 1937) algorithm suggests that we might expect platy morphology for (**I**), with {100} as the major faces. A 4th-order spherical harmonic model was included in the refinement. The texture index was 1.140 (6), indicating that the preferred orientation was significant in this rotated capillary specimen.

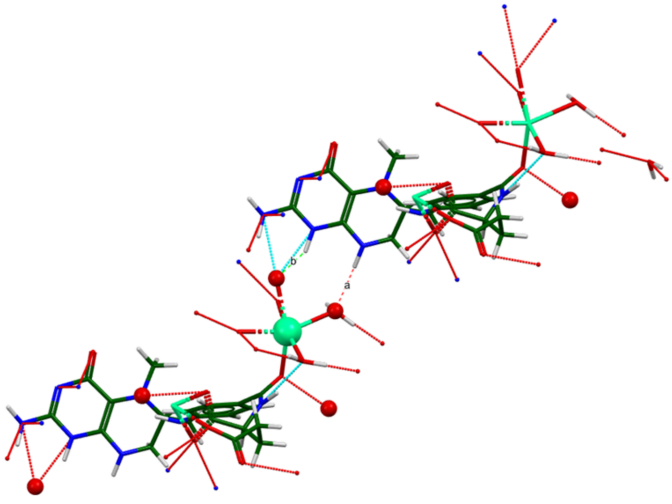

Figure 12
The $R_2^2(8)$ pattern that links the Ca^{2+} cations and the tetrahydropteridin ring system.

Table 2
Experimental details.

	(I)
Crystal data	
Chemical formula	$[Ca(C_{20}H_{23}N_7O_6)(H_2O)_2]\cdot H_2O$
M_r	551.57
Crystal system, space group	Monoclinic, $P2_1/c$
Temperature (K)	295
a, b, c (Å)	16.462 (2), 11.2800 (4), 15.431 (2)
β (°)	117.854 (4)
V (Å^3)	2533.30 (9)
Z	4
Radiation type	Synchotron, λ = 0.41369 Å
μ (mm^{-1})	0.02
Specimen shape, size (mm)	Cylinder, 3 × 1.5
Data collection	
Diffractometer	11-BM APS
Specimen mounting	Kapton capillary
Data collection mode	Transmission
Scan method	Step
2θ values (°)	$2\theta_{min}$ = 0.500 $2\theta_{max}$ = 49.989 $2\theta_{step}$ = 0.001
Refinement	
R factors and goodness of fit	R_p = 0.061, R_{wp} = 0.081, R_{exp} = 0.054, $R(F^2)$ = 0.20984, χ^2 = 2.766
No. of parameters	152
No. of restraints	106
$(\Delta/\sigma)_{max}$	0.562

Computer programs: *GSAS-II* (Toby & Von Dreele, 2013), *DIAMOND* (Putz & Brandenburg, 2025) and *Mercury* (Macrae *et al.*, 2020).

4. Database survey

A connectivity search of the anion in the Cambridge Structural Database (CSD, Version 2025.2.0; Groom *et al.*, 2016) yielded no hits; our structure of Type I (Kaduk *et al.*, 2023) is not yet in the CSD. The powder pattern of Type I is included in the Powder Diffraction File (Kabekkodu *et al.*, 2024) as entry 00-074-0084. A reduced cell search in the CSD yielded seven hits, but no structures for folate or its derivatives.

5. Synthesis and crystallization

The compound stated to be enantiopure calcium L-5-methyltetrahydrofolate trihydrate (batch #414012519), synthesized by Allastir Private Limited, was supplied by Virtus Pharmaceuticals and used as received.

6. Refinement

Crystal data, data collection and structure refinement details are summarized in Table 2.

The pale-yellow powder was packed into a 1.5 mm diameter Kapton capillary, and rotated during the measurement at ~50 Hz. The powder pattern was measured at 295 K at beam line 11-BM (Lee *et al.*, 2008, Wang *et al.*, 2008, Antao *et al.*, 2008) of the Advanced Photon Source at Argonne National Laboratory using a wavelength of 0.413691 (2) Å from 0.5–50° 2θ with a step size of 0.001° and a counting time of 0.1 sec step^{-1}. The high-resolution powder diffraction data were collected using twelve silicon crystal analyzers that allow for

high angular resolution, high precision, and accurate peak positions. A mixture of silicon (NIST SRM 640c) and alumina (NIST SRM 676a) standards (ratio Al_2O_3:Si = 2:1 by weight) was used to calibrate the instrument and refine the monochromatic wavelength used in the experiment. The synchrotron pattern was indexed both by *JADE Pro* (MDI, 2025) and *N-TREOR* (Altomare *et al.*, 2013) on a similar primitive monoclinic unit cell having a = 16.4341, b = 11.2869, c = 15.4326 Å, β = 117.74°, V = 2533.6 Å^3, and Z = 4. The space group suggested by both programs was $P2_1/c$, which was confirmed by successful solution and refinement of the structure.

Attempts to solve the structure by Monte Carlo simulated annealing techniques using a Ca atom, a levomefolate anion from the Kaduk *et al.* (2023) structure, and three O atoms (water molecules) as fragments in several programs were unsuccessful, yielding solutions with severe molecular overlap and/or unreasonable conformations. What turned out to be successful was to use a Ca–levomefolate fragment from the previous structure (chelated through O3 and O4) and three O atoms as fragments in *EXPO2014* (Altomare *et al.*, 2013). Although this structure had two close intermolecular contacts, it was used to begin refinement.

In the initial refinement O59 and O60 moved too close to O6 and so were removed from the model, and the N13···O3 short contact was still present. A new O59 was placed in the void in the structure; it again moved too close to O6 and was removed from the model. O58 was placed at its original position bound to the Ca, and O59 and O60 were placed in two new voids. After recalculation of the H-atom positions in *Materials Studio* (Dassault Systèmes, 2024), O60 was too close to the anion, and was relocated in a new void. Refinement of this model yielded a negative occupancy for O59 and O60 too close to the anion. Both were removed from the model.

The arrangement of the Ca cations suggested the possibility that they were bridged by two symmetry-equivalent water molecules. A search of this connectivity in the CSD yielded 44 hits, so this arrangement is not unprecedented. Optimization of this dihydrate model first using the Forcite module of *Materials Studio* and then *VASP* broke one of the bridging Ca—O bonds (yielding two monodentate water molecules) and moved the dicarboxylate side chain of the anion much more than usual, yielded a tris-chelated anion. The poor agreement of the refined and optimized structure, as well as poorer agreement with the diffraction data, led us to abandon this dihydrate model. The trihydrate structure (two coordinated water molecules and one zeolitic) was optimized with *VASP*.

Rietveld refinement of the *VASP*-optimized trihydrate structure was carried out with *GSAS-II* (Toby & Von Dreele, 2013). Only the 1.0–14.0° portion of the pattern was included in the refinements (d_{min} = 1.697 Å). All non-H atom bond distances and angles were subjected to restraints, based on a *Mercury*/Mogul Geometry Check (Sykes *et al.*, 2011; Bruno *et al.*, 2004). The Mogul average and standard deviation for each quantity were used as the restraint parameters. The phenyl ring was restrained to be planar. The restraints contributed 18.3% to the overall χ^2. The hydrogen atoms were included in calculated positions, which were recalculated during the refinement using *Materials Studio* (Dassault Systèmes, 2024). The U_{iso} values for the heavy atoms were grouped by chemical similarity. For N9 and C16, they refined to slightly negative values, so these were fixed at a reasonable value. The U_{iso} values for the hydrogen atoms were fixed at the value of the heavy atoms to which they are attached. The peak profiles were described using the generalized microstrain model (Stephens, 1999). The background was modeled using a six-term shifted Chebyshev polynomial, with peaks at 1.54, 4.85, and 6.90° to model the scattering from the Kapton capillary and any amorphous component of the sample.

The final refinement of 152 variables using 13,002 observations and 106 restraints yielded the residuals R_{wp} = 0.089 and GOF = 1.66. The largest peak (1.59 Å from C24) and hole (1.57 Å from C19) in the difference-Fourier map are 0.24 (7) and −0.28 (7) e Å^{-3}, respectively. The final Rietveld plot is shown in Fig. 13. The largest features in the normalized error plot are the intensities of the 320 peak at 6.45° and the $13\overline{2}$ peak at 7.02°.

The crystal structure of racemic calcium 5-methyltetrahydrofolate trihydrate was optimized (fixed experimental unit cell) with density functional techniques using *VASP* (Kresse & Furthmüller, 1996) through the *MedeA* graphical interface (Materials Design, 2024). The calculation was carried out on 32 cores of a 144-core (768 Gb memory) HPE Superdome Flex 280 Linux server at North Central College. The calculation used the GGA-PBE functional, a plane wave cutoff energy of 400.0 eV, and a k-point spacing of 0.5 Å^{-1} leading to a 1 × 2 × 1 mesh, and took ∼26.2 h. Single-point density functional calculations (fixed experimental cell) and population analysis were carried out using *CRYSTAL23* (Erba *et al.*, 2023). The basis sets for the H, C, N, and O atoms in the calculation were those of Gatti *et al.* (1994), and that for Ca was that of Peintinger *et al.* (2013). The calculations were run on a 3.5 GHz PC using 8 k-points and the B3LYP functional, and took about 4.0 h.

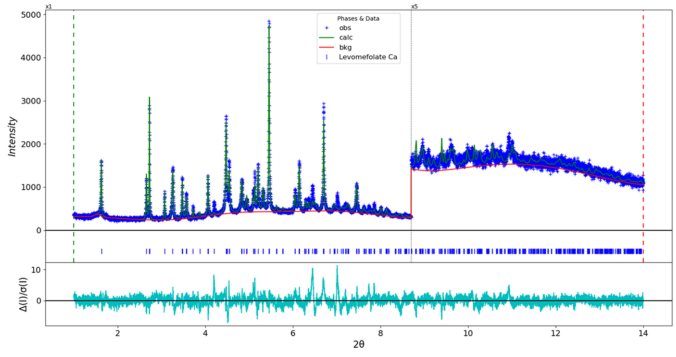

Figure 13
The difference plot for the Rietveld refinement of (**I**). The blue crosses represent the observed data points, and the green line is the calculated pattern. The cyan curve is the normalized error plot, and the red line is the background curve. The blue tick marks indicate the peak positions. The vertical scale has been multiplied by a factor of 5 for 2θ > 8.7°.

Acknowledgements

Use of the Advanced Photon Source at Argonne National Laboratory was supported by the US Department of Energy, Office of Science, Office of Basic Energy Sciences, under Contract No. DE-AC02–06CH11357. We thank Saul Lapidus for his assistance in the data collection, and Andrew Rosenthal of Virtus Pharmaceuticals for supplying the sample.

References

Acharya, S. N. G., Venkatesan, K., Bhattacharya, S., Gopalan, R. S. & Kulkarni, G. U. (2000). *Chem. Commun.* pp. 1351–1352.

Altomare, A., Cuocci, C., Giacovazzo, C., Moliterni, A., Rizzi, R., Corriero, N. & Falcicchio, A. (2013). *J. Appl. Cryst.* **46**, 1231–1235.

Antao, S. M., Hassan, I., Wang, J., Lee, P. L. & Toby, B. H. (2008). *Can. Mineral.* **46**, 1501–1509.

Bravais, A. (1866). *Etudes Cristallographiques*. Paris: Gauthier Villars.

Bruno, I. J., Cole, J. C., Kessler, M., Luo, J., Motherwell, W. D. S., Purkis, L. H., Smith, B. R., Taylor, R., Cooper, R. I., Harris, S. E. & Orpen, A. G. (2004). *J. Chem. Inf. Comput. Sci.* **44**, 2133–2144.

Cotter, J., Hogan, A. L. & O'Shea, D. F. (2007). *Org. Lett.* **9**, 1493–1496.

Das, D. (2019). *ChemistrySelect* **4**, 1428–1436.

Dassault Systèmes. (2024). *Materials Studio 2025*. BIOVIA, San Diego, USA.

Donnay, J. D. H. & Harker, D. (1937). *Am. Mineral.* **22**, 446–467.

Erba, A., Desmarais, J. K., Casassa, S., Civalleri, B., Donà, L., Bush, I. J., Searle, B., Maschio, L., Edith-Daga, L., Cossard, A., Ribaldone, C., Ascrizzi, E., Marana, N. L., Flament, J.-P. & Kirtman, B. (2023). *J. Chem. Theory Comput.* **19**, 6891–6932.

Etter, M. C. (1990). *Acc. Chem. Res.* **23**, 120–126.

Favre-Nicolin, V. & Černý, R. (2002). *J. Appl. Cryst.* **35**, 734–743.

Friedel, G. (1907). *Bull. Soc. Française Minéral.* **30**, 326-455.

Gatti, C., Saunders, V. R. & Roetti, C. (1994). *J. Chem. Phys.* **101**, 10686–10696.

Groom, C. R., Bruno, I. J., Lightfoot, M. P. & Ward, S. C. (2016). *Acta Cryst.* B**72**, 171–179.

Hong, Y., Yufit, D. S., Letzelter, N. & Steed, J. W. (2020). *CrystEngComm* **22**, 2585–2592.

Kabekkodu, S., Dosen, A. & Blanton, T. N. (2024). *Powder Diffr.* **39**, 47–59.

Kaduk, J. A., Patel, N. V. & Golab, J. T. (2023). *Powder Diffr.* **38**, 207–214.

Kresse, G. & Furthmüller, J. (1996). *Comput. Mater. Sci.* **6**, 15–50.

Lee, P. L., Shu, D., Ramanathan, M., Preissner, C., Wang, J., Beno, M. A., Von Dreele, R. B., Ribaud, L., Kurtz, C., Antao, S. M., Jiao, X. & Toby, B. H. (2008). *J. Synchrotron Rad.* **15**, 427–432.

Macrae, C. F., Sovago, I., Cottrell, S. J., Galek, P. T. A., McCabe, P., Pidcock, E., Platings, M., Shields, G. P., Stevens, J. S., Towler, M. & Wood, P. A. (2020). *J. Appl. Cryst.* **53**, 226–235.

Materials Design. (2024). *MedeA 3.7.2*. Materials Design Inc., San Diego, USA.

MDI. (2025). *JADE Pro version 9.3*. Materials Data, Livermore, USA.

Müller, R., Moser, R. & Egger, T. (2002). US Patent 6,441,168 B1.

Okamura, T., Furuya, R. & Onitsuka, K. (2015). *Dalton Trans.* **44**, 7512–7523.

Peintinger, M. F., Oliveira, D. V. & Bredow, T. (2013). *J. Comput. Chem.* **34**, 451–459.

Putz, H. & Brandenburg, K. (2025). *DIAMOND*. Crystal Impact, Bonn, Germany.

Rammohan, A. & Kaduk, J. A. (2018). *Acta Cryst.* B**74**, 239–252.

Silk Scientific. (2013). *UN-SCAN-IT 7.0*. Silk Scientific Corporation, Oren UT.

Stephens, P. W. (1999). *J. Appl. Cryst.* **32**, 281–289.

Streek, J. van de & Neumann, M. A. (2014). *Acta Cryst.* B**70**, 1020–1032.

Sykes, R. A., McCabe, P., Allen, F. H., Battle, G. M., Bruno, I. J. & Wood, P. A. (2011). *J. Appl. Cryst.* **44**, 882–886.

Toby, B. H. & Von Dreele, R. B. (2013). *J. Appl. Cryst.* **46**, 544–549.

Wang, J., Toby, B. H., Lee, P. L., Ribaud, L., Antao, S. M., Kurtz, C., Ramanathan, M., Von Dreele, R. B. & Beno, M. A. (2008). *Rev. Sci. Instrum.* **79**, 085105.

Wavefunction, Inc. (2025). *Spartan '24. V. 1.3.1*. Wavefunction Inc., Irvine, CA.

Wheatley, A. M. & Kaduk, J. A. (2019). *Powder Diffr.* **34**, 35–43.

supporting information

Acta Cryst. (2026). E**82**, 33-39 [https://doi.org/10.1107/S2056989025010515]

Structure of racemic calcium 5-methyltetrahydrofolate trihydrate from synchrotron powder diffraction data and density functional theory

Jacob K. Salazar and James A. Kaduk

Computing details

(I)

Crystal data

$C_{20}H_{29}CaN_7O_9$
M_r = 551.57
Monoclinic, $P2_1/c$
a = 16.462 (2) Å
b = 11.2800 (4) Å
c = 15.431 (2) Å
β = 117.854 (4)°
V = 2533.30 (9) Å^3
Z = 4
D_x = 1.446 Mg m^{-3}
Synchotron radiation, λ = 0.41369 Å
μ = 0.02 mm^{-1}
T = 295 K
cylinder, 3 × 1.5 mm

Data collection

11-BM APS diffractometer
Specimen mounting: Kapton capillary
Data collection mode: transmission
Scan method: step
$2\theta_{min}$ = 0.500°, $2\theta_{max}$ = 49.989°, $2\theta_{step}$ = 0.001°

Refinement

Least-squares matrix: full
R_p = 0.061
R_{wp} = 0.080
R_{exp} = 0.054
$R(F^2)$ = 0.20984
49497 data points
Profile function: Finger-Cox-Jephcoat function parameters U, V, W, X, Y, SH/L: peak variance(Gauss) = Utan(Th)^2+Vtan(Th)+W: peak HW(Lorentz) = X/cos(Th)+Ytan(Th); SH/L = S/L+H/L U, V, W in (centideg)^2, X & Y in centideg 1.163, -0.126, 0.063, 0.000, 0.000, 0.002,
152 parameters
106 restraints
28 constraints
Weighting scheme based on measured s.u.'s
$(\Delta/\sigma)_{max}$ = 0.562
Background function: Background function: "chebyschev-1" function with 6 terms: 221(3), 6.1(20), 61(5), -88(3), -17.5(18), 28.1(21), Background peak parameters: pos, int, sig, gam: 4.85(6), 7.5(5)e4, 9.8(6)e3, 0.100, 6.90(6), 7.7(6)e4, 1.04(7)e4, 0.100, 1.542(8), 1.17(13)e3, 49(10), 0.100,
Preferred orientation correction: Simple spherical harmonic correction Order = 4 Coefficients: 0:0:C(2,-2) = 0.097(18); 0:0:C(2,0) = -0.310(20); 0:0:C(2,2) = -0.224(25); 0:0:C(4,-4) = -0.788(25); 0:0:C(4,-2) = 0.152(21); 0:0:C(4,0) = -0.565(24); 0:0:C(4,2) = -0.093(29); 0:0:C(4,4) = -0.106(28)

Fractional atomic coordinates and isotropic or equivalent isotropic displacement parameters (Å^2)

	x	y	z	U_{iso}*/U_{eq}
O1	0.0612 (13)	0.654 (2)	0.9996 (8)	0.086 (7)*

O2	0.3927 (14)	0.4819 (15)	0.5608 (15)	0.353 (12)*
O3	0.3201 (13)	0.0703 (17)	0.7151 (16)	0.353 (12)*
O4	0.4513 (14)	0.1719 (17)	0.7822 (12)	0.353 (12)*
O5	0.4693 (18)	−0.095 (2)	0.6667 (14)	0.353 (12)*
O6	0.420 (3)	−0.1450 (18)	0.5111 (16)	0.353 (12)*
N7	0.0588 (8)	0.7359 (10)	0.8125 (8)	0.086 (7)*
N8	−0.1186 (9)	0.7459 (15)	0.6733 (10)	0.086 (7)*
N9	0.1252 (12)	0.5511 (15)	0.7411 (13)	0.0800*
N10	−0.1617 (7)	0.6105 (17)	0.7545 (12)	0.086 (7)*
N11	−0.0516 (11)	0.5285 (12)	0.9040 (11)	0.086 (7)*
N12	0.4084 (13)	0.2978 (14)	0.6214 (18)	0.353 (12)*
N13	−0.2048 (13)	0.481 (2)	0.8413 (19)	0.086 (7)*
C14	0.0421 (9)	0.7403 (15)	0.7101 (9)	0.086 (7)*
C15	−0.0510 (12)	0.7969 (18)	0.6481 (12)	0.086 (7)*
C16	0.0457 (10)	0.618 (2)	0.6735 (11)	0.0800*
C17	−0.0086 (7)	0.6796 (14)	0.8253 (7)	0.086 (7)*
C18	−0.0929 (7)	0.6668 (11)	0.7448 (7)	0.086 (7)*
C19	0.1103 (19)	0.836 (2)	0.8741 (16)	0.086 (7)*
C20	0.0119 (10)	0.6152 (14)	0.9164 (7)	0.086 (7)*
C21	0.1867 (10)	0.514 (3)	0.7123 (14)	0.307 (14)*
C22	−0.1376 (10)	0.540 (2)	0.8344 (15)	0.086 (7)*
C23	0.2803 (10)	0.519 (6)	0.7755 (17)	0.307 (14)*
C24	0.1562 (12)	0.475 (5)	0.6169 (15)	0.307 (14)*
C25	0.3492 (13)	0.1977 (15)	0.6108 (13)	0.353 (12)*
C26	0.3120 (13)	0.442 (2)	0.6485 (16)	0.307 (14)*
C27	0.345 (2)	0.109 (2)	0.5327 (12)	0.353 (12)*
C28	0.3422 (11)	0.480 (5)	0.7446 (16)	0.307 (14)*
C29	0.2183 (14)	0.443 (5)	0.5847 (18)	0.307 (14)*
C30	0.3781 (17)	0.4084 (14)	0.6120 (18)	0.353 (12)*
C31	0.439 (2)	0.0578 (16)	0.552 (2)	0.353 (12)*
C32	0.3787 (14)	0.1371 (18)	0.7102 (12)	0.353 (12)*
C33	0.4518 (16)	−0.0721 (16)	0.5796 (14)	0.353 (12)*
H35	−0.19170	0.77330	0.63258	0.0860*
H36	0.13503	0.53082	0.81578	0.0800*
H37	−0.23431	0.62330	0.69841	0.0860*
H38	0.48079	0.28272	0.63774	0.3530*
H39	−0.26479	0.47245	0.76741	0.0860*
H40	−0.22538	0.53023	0.89017	0.0860*
H41	0.09738	0.79731	0.70599	0.0860*
H42	−0.04601	0.89647	0.66233	0.0860*
H43	−0.07304	0.78004	0.56729	0.0860*
H44	−0.01902	0.56744	0.66078	0.0800*
H45	0.04698	0.62727	0.60060	0.0800*
H46	0.06109	0.89824	0.88506	0.0860*
H47	0.14541	0.88674	0.83676	0.0860*
H48	0.16439	0.80226	0.94830	0.0860*
H49	0.30626	0.55502	0.85297	0.3070*
H50	0.07940	0.46907	0.56474	0.3070*

H51	0.27683	0.23374	0.58496	0.3530*
H52	0.31251	0.15519	0.45838	0.3530*
H53	0.29985	0.03045	0.52912	0.3530*
H54	0.41885	0.47878	0.79795	0.3070*
H55	0.19196	0.41720	0.50459	0.3070*
H56	0.44720	0.06720	0.48279	0.3530*
H60	0.49554	0.11077	0.61325	0.3530*
Ca34	0.5495 (10)	0.4654 (11)	0.6731 (10)	0.339 (13)*
O57	0.6087 (18)	0.5830 (18)	0.5584 (19)	0.0879*
H61	0.60810	0.55340	0.50400	0.0879*
H62	0.61710	0.65090	0.59210	0.0879*
O59	0.5736 (15)	0.2707 (16)	0.6397 (16)	0.0879*
H65	0.59890	0.25060	0.70350	0.0879*
H66	0.57580	0.22990	0.59080	0.0879*
O58	0.356 (3)	0.785 (3)	0.182 (3)	0.0879*
H63	0.31080	0.83930	0.16760	0.0879*
H64	0.39050	0.72700	0.17760	0.0879*

Geometric parameters (Å, º)

O1—C20	1.235 (3)	C27—C31	1.545 (5)
O2—C30	1.243 (2)	C27—H52	1.14 (2)
O2—Ca34	2.351 (16)	C27—H53	1.14 (3)
O2—H61^{i}	1.07 (2)	C28—C23	1.386 (4)
O3—C32	1.254 (4)	C28—C26	1.393 (3)
O3—H40^{ii}	1.71 (2)	C28—H54	1.140 (15)
O3—Ca34^{iii}	2.350 (14)	C29—C24	1.378 (4)
O4—C32	1.256 (4)	C29—C26	1.389 (3)
O4—Ca34^{iii}	2.431 (14)	C29—H55	1.139 (15)
O5—C33	1.263 (4)	C30—O2	1.243 (2)
O5—Ca34^{iii}	2.718 (15)	C30—N12	1.326 (5)
O6—C33	1.246 (4)	C30—C26	1.489 (3)
N7—C14	1.473 (2)	C30—Ca34	2.60 (2)
N7—C17	1.370 (4)	C31—C27	1.545 (5)
N7—C19	1.468 (3)	C31—C33	1.514 (3)
N8—C15	1.4582 (17)	C31—H56	1.14 (2)
N8—C18	1.3248 (17)	C31—H60	1.14 (3)
N8—H35	1.110 (11)	C32—O3	1.254 (4)
N9—C16	1.445 (3)	C32—O4	1.256 (4)
N9—C21	1.347 (5)	C32—C25	1.536 (3)
N9—H36	1.110 (16)	C32—Ca34^{iii}	2.530 (18)
N10—C18	1.368 (3)	C33—O5	1.263 (4)
N10—C22	1.364 (4)	C33—O6	1.246 (4)
N10—H37	1.110 (11)	C33—C31	1.514 (3)
N11—C20	1.379 (3)	H35—N8	1.110 (11)
N11—C22	1.323 (4)	H36—N9	1.110 (16)
N12—C25	1.450 (3)	H37—N10	1.110 (11)
N12—C30	1.326 (5)	H38—N12	1.110 (17)

N12—H38	1.110 (17)	H38—O59	1.52 (2)
N13—C22	1.336 (4)	H39—N13	1.11 (2)
N13—H39	1.11 (2)	H40—O3^{iv}	1.71 (2)
N13—H40	1.11 (3)	H40—N13	1.11 (3)
C14—N7	1.473 (2)	H41—C14	1.141 (11)
C14—C15	1.5164 (18)	H42—C15	1.14 (2)
C14—C16	1.506 (6)	H43—C15	1.140 (18)
C14—H41	1.141 (11)	H44—C16	1.140 (19)
C15—N8	1.4582 (17)	H45—C16	1.140 (18)
C15—C14	1.5164 (18)	H46—C19	1.14 (3)
C15—H42	1.14 (2)	H47—C19	1.14 (2)
C15—H43	1.140 (18)	H48—C19	1.14 (3)
C16—N9	1.445 (3)	H49—C23	1.140 (15)
C16—C14	1.506 (6)	H50—C24	1.140 (16)
C16—H44	1.140 (19)	H51—C25	1.14 (2)
C16—H45	1.140 (18)	H52—C27	1.14 (2)
C17—N7	1.370 (4)	H53—C27	1.14 (3)
C17—C18	1.370 (5)	H54—C28	1.140 (15)
C17—C20	1.474 (6)	H55—C29	1.139 (15)
C18—N8	1.3248 (17)	H56—C31	1.14 (2)
C18—N10	1.368 (3)	H60—C31	1.14 (3)
C18—C17	1.370 (5)	Ca34—O2	2.351 (16)
C19—N7	1.468 (3)	Ca34—O3^{v}	2.350 (14)
C19—H46	1.14 (3)	Ca34—O4^{v}	2.431 (14)
C19—H47	1.14 (2)	Ca34—O5^{v}	2.718 (15)
C19—H48	1.14 (3)	Ca34—C30	2.60 (2)
C20—O1	1.235 (3)	Ca34—C32^{v}	2.530 (18)
C20—N11	1.379 (3)	Ca34—O57	2.729 (14)
C20—C17	1.474 (6)	Ca34—O59	2.332 (14)
C21—N9	1.347 (5)	O57—Ca34	2.729 (14)
C21—C23	1.387 (3)	O57—H61	0.90 (2)
C21—C24	1.388 (3)	O57—H62	0.90 (2)
C22—N10	1.364 (4)	H61—O2^{i}	1.07 (2)
C22—N11	1.323 (4)	H61—O57	0.90 (2)
C22—N13	1.336 (4)	H62—O57	0.90 (2)
C23—C21	1.387 (3)	O59—H38	1.52 (2)
C23—C28	1.386 (4)	O59—Ca34	2.332 (14)
C23—H49	1.140 (15)	O59—H65	0.90 (2)
C24—C21	1.388 (3)	O59—H66	0.900 (19)
C24—C29	1.378 (4)	H65—O59	0.90 (2)
C24—H50	1.140 (16)	H65—H66	1.6141
C25—N12	1.450 (3)	H65—O58^{i}	1.61 (3)
C25—C27	1.543 (4)	H66—O59	0.900 (19)
C25—C32	1.536 (3)	H66—H65	1.6141
C25—H51	1.14 (2)	O58—H65^{i}	1.61 (3)
C26—C28	1.393 (3)	O58—H63	0.90 (3)
C26—C29	1.389 (3)	O58—H64	0.90 (3)
C26—C30	1.489 (3)	H63—O58	0.90 (3)

C27—C25	1.543 (4)	H64—O58	0.90 (3)

C30—O2—Ca34	87.1 (12)	N10—C22—N11	122.6 (2)
C30—O2—H61^{i}	115.0 (15)	N10—C22—N13	117.4 (3)
Ca34—O2—H61^{i}	100.9 (12)	N11—C22—N13	120.0 (3)
C32—O3—Ca34^{iii}	83.2 (9)	C21—C23—C28	120.0 (4)
C14—N7—C17	114.3 (4)	C21—C23—H49	120.0 (10)
C14—N7—C19	115.5 (5)	C28—C23—H49	119.9 (10)
C17—N7—C19	121.8 (6)	C21—C24—C29	120.3 (3)
C15—N8—C18	120.1 (3)	C21—C24—H50	120.0 (11)
C15—N8—H35	120.0 (9)	C29—C24—H50	119.7 (12)
C18—N8—H35	120.0 (9)	N12—C25—C27	112.1 (3)
C16—N9—C21	119.3 (4)	N12—C25—C32	110.7 (3)
C16—N9—H36	120.0 (14)	C27—C25—C32	111.6 (5)
C21—N9—H36	120.7 (14)	N12—C25—H51	107.4 (11)
C18—N10—C22	117.7 (3)	C27—C25—H51	107.4 (13)
C18—N10—H37	120.0 (9)	C32—C25—H51	107.4 (13)
C22—N10—H37	122.3 (9)	C28—C26—C29	118.58 (17)
C20—N11—C22	120.0 (4)	C28—C26—C30	121.3 (4)
C25—N12—C30	121.4 (4)	C29—C26—C30	120.0 (4)
C25—N12—H38	120.0 (11)	C25—C27—C31	114.7 (4)
C30—N12—H38	118.5 (12)	C25—C27—H52	108.6 (15)
C22—N13—H39	109.4 (12)	C31—C27—H52	109 (3)
C22—N13—H40	110 (3)	C25—C27—H53	109.5 (16)
H39—N13—H40	109.5 (19)	C31—C27—H53	106.9 (14)
N7—C14—C15	108.57 (18)	H52—C27—H53	108.5 (18)
N7—C14—C16	110.57 (14)	C23—C28—C26	120.7 (3)
C15—C14—C16	110.9 (2)	C23—C28—H54	119.9 (11)
N7—C14—H41	108.9 (10)	C26—C28—H54	119.4 (12)
C15—C14—H41	108.9 (11)	C24—C29—C26	120.8 (3)
C16—C14—H41	108.9 (13)	C24—C29—H55	119.2 (14)
N8—C15—C14	109.7 (2)	C26—C29—H55	120.1 (14)
N8—C15—H42	109.4 (15)	O2—C30—N12	121.5 (3)
C14—C15—H42	109.4 (12)	O2—C30—C26	117.6 (3)
N8—C15—H43	109.5 (15)	N12—C30—C26	120.0 (5)
C14—C15—H43	109.4 (11)	C27—C31—C33	114.3 (5)
H42—C15—H43	109.4 (7)	C27—C31—H56	110 (3)
N9—C16—C14	112.9 (4)	C33—C31—H56	107.0 (13)
N9—C16—H44	108.9 (19)	C27—C31—H60	108.6 (12)
C14—C16—H44	108.9 (9)	C33—C31—H60	109 (2)
N9—C16—H45	109.5 (12)	H56—C31—H60	108.7 (15)
C14—C16—H45	107.8 (17)	O3—C32—O4	125.1 (4)
H44—C16—H45	108.9 (10)	O3—C32—C25	115.8 (4)
N7—C17—C18	117.6 (2)	O4—C32—C25	118.0 (3)
N7—C17—C20	121.7 (3)	O5—C33—O6	124.1 (4)
C18—C17—C20	119.76 (18)	O5—C33—C31	115.7 (4)
N8—C18—N10	116.4 (3)	O6—C33—C31	116.8 (4)
N8—C18—C17	118.6 (4)	N12—H38—Ca34	105.9 (10)

N10—C18—C17	119.3 (2)	O2—Ca34—O3^{v}	144.4 (5)
N7—C19—H46	109.5 (17)	O2—Ca34—H38	69.2 (4)
N7—C19—H47	109.4 (11)	O3^{v}—Ca34—H38	143.9 (6)
H46—C19—H47	110 (2)	O2—Ca34—O59	98.8 (5)
N7—C19—H48	109.4 (18)	O3^{v}—Ca34—O59	116.4 (5)
H46—C19—H48	109.6 (15)	H38—Ca34—O59	38.4 (5)
H47—C19—H48	109 (2)	H61—O57—H62	142 (2)
O1—C20—N11	118.8 (3)	O2^{i}—H61—O57	179.9 (13)
O1—C20—C17	124.4 (6)	Ca34—O59—H65	92.0 (12)
N11—C20—C17	113.3 (3)	Ca34—O59—H66	138.1 (17)
N9—C21—C23	121.0 (3)	H65—O59—H66	128 (2)
N9—C21—C24	119.5 (3)	H63—O58—H64	163 (4)
C23—C21—C24	119.41 (16)		

Symmetry codes: (i) −*x*+1, −*y*+1, −*z*+1; (ii) −*x*, *y*−1/2, −*z*+3/2; (iii) −*x*+1, *y*−1/2, −*z*+3/2; (iv) −*x*, *y*+1/2, −*z*+3/2; (v) −*x*+1, *y*+1/2, −*z*+3/2.

Poly[[(*μ*-(2*S*)-2-{[4-({[(6*S*)-2-amino-5-methyl-1,4,5,6,7,8-hexahydropteridin-6-yl]methyl}amino)phenyl]formamido}pentanedioato)diaquacalcium(II)] monohydrate] (I_VASP)

Crystal data

$[Ca(C_{20}H_{23}N_7O_6)(H_2O)_2]\cdot H_2O$
M_r = 551.57
Monoclinic, $P2_1/c$
a = 16.4610 Å
b = 11.2801 Å
c = 15.4287 Å
β = 117.86°
V = 2532.84 Å^3
Z = 4
T = 295 K

Data collection

$h = \rightarrow$
$k = \rightarrow$
$l = \rightarrow$

Fractional atomic coordinates and isotropic or equivalent isotropic displacement parameters (Å^2)

	x	y	z	B_{iso}*/B_{eq}
O1	0.13566	0.70774	1.00951	
O2	0.41966	0.42136	0.58093	
O3	0.29242	−0.00251	0.67295	
O4	0.42010	0.10694	0.75199	
O5	0.43639	−0.17961	0.69842	
O6	0.39155	−0.25179	0.54798	
N7	0.05880	0.68205	0.79615	
N8	−0.11769	0.58664	0.70651	
N9	0.09150	0.52271	0.67370	
N10	−0.12035	0.58077	0.85798	
N11	0.00194	0.64850	1.00439	
N12	0.39032	0.22700	0.58383	
N13	−0.12688	0.56526	1.00539	
C14	0.00480	0.69869	0.68938	
C15	−0.09826	0.67389	0.64879	
C16	0.05100	0.63726	0.63436	
C17	0.01069	0.66421	0.85097	

C18	−0.07577	0.61244	0.80519
C19	0.13942	0.76049	0.83468
C20	0.05307	0.67737	0.95737
C21	0.15616	0.47466	0.65244
C22	−0.07910	0.59947	0.95634
C23	0.20736	0.37338	0.70253
C24	0.17614	0.52626	0.58049
C25	0.33511	0.12286	0.57521
C26	0.29356	0.37675	0.60998
C27	0.35398	0.02425	0.51743
C28	0.27321	0.32543	0.68094
C29	0.24465	0.47964	0.56231
C30	0.37015	0.34014	0.59206
C31	0.44264	−0.04915	0.57708
C32	0.35019	0.07457	0.67412
C33	0.42236	−0.16853	0.60989
H35	−0.18561	0.56359	0.67704
H36	0.09276	0.50005	0.73826
H37	−0.18480	0.54237	0.82579
H38	0.45058	0.21627	0.57917
H39	−0.17049	0.49511	0.97330
H40	−0.08332	0.55098	1.07772
H41	0.00844	0.79356	0.67308
H42	−0.13291	0.75868	0.64695
H43	−0.12671	0.64234	0.57308
H44	−0.00037	0.62877	0.55666
H45	0.10382	0.69757	0.63470
H46	0.11872	0.85487	0.82828
H47	0.17518	0.74691	0.79055
H48	0.18556	0.74050	0.91150
H49	0.19554	0.33384	0.76029
H50	0.14189	0.60725	0.54241
H51	0.26219	0.14818	0.53432
H52	0.35647	0.06664	0.45434
H53	0.29437	−0.03566	0.48652
H54	0.31436	0.25156	0.72465
H55	0.26225	0.52604	0.51125
H56	0.47397	−0.06874	0.52950
H60	0.49337	0.00057	0.64075
Ca34	0.57864	0.41693	0.68106
O57	0.64519	0.54999	0.60875
H61	0.62494	0.61942	0.63160
H62	0.61835	0.55840	0.53548
O59	0.57705	0.24688	0.59726
H65	0.60649	0.18401	0.64869
H66	0.59473	0.24136	0.54090
O58	0.37907	0.88448	0.24975
H63	0.32047	0.91148	0.19674

H64	0.40245	0.82484	0.21898

Hydrogen-bond geometry (Å, º)

D—H···*A*	*D*—H	H···*A*	*D*···*A*	*D*—H···*A*
N8—H35···O57^{i}	1.02	2.48	3.490	169
N10—H37···O3^{ii}	1.03	1.85	2.805	152
N12—H38···O59	1.03	2.00	2.991	160
N13—H39···O3^{ii}	1.03	2.21	2.928	125
N13—H39···O1^{iii}	1.03	2.34	3.086	128
O57—H61···O4^{iv}	0.98	2.24	2.888	122
O57—H62···O2^{v}	1.01	1.62	2.625	176
O58—H64···O5^{vi}	1.00	1.81	2.749	156
O59—H65···O58^{v}	1.00	1.66	2.588	151
O59—H66···O6^{vii}	1.04	1.49	2.525	170
C16—H45···O1^{viii}	1.10	2.47	3.349	136
C19—H48···O1	1.09	2.06	2.791	121
C24—H50···O1^{viii}	1.09	2.14	3.157	154
C25—H51···N13^{ix}	1.10	2.22	3.120	137
C28—H54···O4	1.09	2.28	3.263	150
C31—H60···O58^{v}	1.10	2.37	3.446	165

Symmetry codes: (i) $x-1$, y, z; (ii) $-x$, $y+1/2$, $-z+3/2$; (iii) $-x$, $-y+1$, $-z+2$; (iv) $-x+1$, $y+1/2$, $-z+3/2$; (v) $-x+1$, $-y+1$, $-z+1$; (vi) x, $-y+1/2$, $z-1/2$; (vii) $-x+1$, $-y$, $-z+1$; (viii) x, $-y+3/2$, $z-1/2$; (ix) $-x$, $y-1/2$, $-z+3/2$.